

Dielectric characteristic and local phase transition of gallium phosphide nanosolid

Zhao-Chun Zhang · Jian-Lin Li

Received: 13 January 2011 / Accepted: 2 March 2011 / Published online: 9 March 2011
© Springer Science+Business Media, LLC 2011

Abstract The dependences of relative dielectric permittivity, ϵ'_r , and tangent of dielectric loss angle, $\operatorname{tg} \delta$, of gallium phosphide (GaP) nanosolid on frequency and temperature were investigated. The GaP nanopowders are subglobular in shape, with the average crystallite size of about 50 nm evaluated from Scherrer equation. It can be concluded that the leakage current mechanism plays an important role in the dielectric loss of the GaP nanosolid. The dielectric characteristic of the GaP nanosolid in the range 298–350 K allows to detect an ϵ'_r or $\operatorname{tg} \delta$ peak at 303 K that is due to local phase transitions, probably in the high hydrostatic stress field of dislocations with an edge component. Under the influence of an electric field, the high hydrostatic stress field of dislocations can undergo changes in deformation, accompanied by drastic stress-induced changes in the order parameter near the phase transition temperature, and hence, changes in the Gibbs free energy per unit volume can be found.

Introduction

In the consolidation of nanopowders to form bulk nanostructured materials, techniques employed to date have been used for reference from the powder metallurgical and ceramic processing industries. Every stage in the consolidation process is important, but the most important

stage is the design and control of nanopowders. The factors of the design and control involve the average particle size, particle size distribution, geometric shape of particles, chemical composition, crystal structure, and defects of nanopowders. On the other hand, it is essential to consider the selection of the most suitable processing route. It is almost universally accepted that the control optimization of compaction and sintering of nanopowders are two important stages [1]. During the compaction of nanopowders the pressure required to produce a high degree of compaction is normally several times the yield stress of the material being compacted. This means that the cold compaction of nanopowders, such as metal nanopowders, is likely to require stresses in the 10^9 Pa range [1]. Sintering of nanopowders can occur when powders are packed together and heated to a temperature, almost much lower than the typical sintering temperature $\sim 2T_m/3$ for the corresponding bulk materials being sintered [1]. But it is unusual to observe rapid low-temperature densification in practice.

In fact, the point we are trying to make is that the nanopowders will undergo a pressing with high pressure and a heat-treatment in the consolidation to form bulk nanostructured materials. Under appropriate conditions, such as temperature, hydrostatic pressure, and other fields, nanomaterial may undergo a transition from one phase to another. Mohanty et al. have presented measurements of the influence of local strain on the phase transition behavior of epitaxial MnAs films on GaAs (001) [2]. Using the internal friction and Young's modulus data, Klimm analyzed the local phase transition in GaP and GaAs [3]. Klimm et al. have measured the complex dielectric permittivity ($\epsilon^* = \epsilon' - i \epsilon''$) of GaP:S samples [4]. The $\epsilon'(T)$ and $\epsilon''(T)$ curves of GaP:S after ultrasonic treatment showed abrupt changes near 303 or 302 K, respectively.

Z.-C. Zhang (✉) · J.-L. Li
School of Materials Science and Engineering,
Shanghai University, Shanghai 200072, China
e-mail: zhangzhaochun@shu.edu.cn

They attributed this dielectric characteristic to the local phase transition that occurred in the stress field of dislocations moved by ultrasonic deformation.

Being different from the above-mentioned experimental observation, this investigation emphasizes that the sample used in this experiment is the GaP nanosolid, a consolidated structure of GaP nanopowders. This could suggest an enrichment investigation on the processing and properties of semiconductor nanomaterials. It is known that extrinsic material properties, such as dielectric loss and electric carrier density, of semiconductor nanosolids are different from those of the corresponding bulk crystals. The grain boundaries and different types of defects in the nanosolids are highly responsible for these extrinsic properties. A remarkable change in the dielectric characteristic attributed to the nanoscale structure, to be specific, can be used to characterize the local phase transition in the high hydrostatic stress field of dislocations with an edge component in the GaP nanosolid. The investigation of local phase transition of nanomaterial is essential for the scientific study of nanomaterial properties and for their use in engineering applications.

Experimental

The GaP nanopowders used in this study was prepared by a benzene-thermal method [5]. In order to remove the survival impurities (sodium chloride and carbon), a slurry of about 2 g of as-prepared GaP nanopowders placed in an Erlenmeyer flask filled with 25 mL water was stirred gently at room temperature for 24 h. Then, it was filtered and dried at 378 K in the air.

The GaP nanosolid was prepared using the traditional powder consolidation method. The as-purified GaP nanopowders of about 1 g was put in the squeezing dies of a squeeze molding machine. The vertical compacting pressure and squeezing time were 5 MPa and 10 s, respectively. Then, both sides of the new-made lump were coated uniformly by a conducting silver slurry. Finally, the lump was heated in air at 723 K for 1 h in a muffle furnace.

The GaP nanopowder was characterized by X-ray diffraction (XRD) using an X-ray diffractometer (D/max-rC) with nickel-filtered Cu $K\alpha$ radiation. Before measurement, the correction for instrumental broadening was carried out by using single crystal silicon as the standard sample. High-resolution transmission electron micrograph (HRTEM) images were recorded on a JEM-2010F microscope operated at 200 kV. The determination of complex dielectric permittivity (ϵ^*) was performed by measurements of the capacity and the loss angle of a capacitor that contained the sample as dielectrics with the HP 4284A Precision LCR-meter.

Results and discussion

Phase analysis by XRD

The XRD pattern of as-purified GaP nanopowders is shown in Fig. 1. The (hkl) values assigned to peaks corresponding to the cubic GaP are in agreement with standard JCPDS values (80-0015). Based on the full width at half maximum of true peak breadth (corrected for instrumental broadening) of the $\{111\}$, $\{220\}$, and $\{311\}$ planes responsible for the diffraction, the coherently diffracting domain size were given 44.2, 55.4, and 51.6 nm, respectively, by the Scherrer equation (the shape factor, $K = 0.89$). In such a case, the average crystallite size of the GaP nanopowders was determined as about 50 nm.

Dependences of ϵ'_r and $\operatorname{tg} \delta$ on f

The dependences of the relative dielectric permittivity, ϵ'_r , and tangent of dielectric loss angle, $\operatorname{tg} \delta$, for the GaP nanosolid on frequency, f , at 298 K are shown in Figs. 2 and 3, respectively. As Fig. 2 shows, for $f < 100$ Hz ϵ'_r decreases rapidly with increasing frequency, and then, much more slowly. In addition, the value of ϵ'_r of the GaP nanosolid at very low frequency is much higher than that of bulk GaP ($\epsilon_0 = 11.02$, at 300 K) [6]. It can be seen from Fig. 3 that in the range 10–10,000 Hz $\operatorname{tg} \delta$ of the GaP nanosolid decreases approximately linearly with increasing frequency. Applying linear regression analysis to the experimental results gives $\operatorname{tg} \delta = -5.39188 \log f + 26.66825$, correlation coefficient $R = 0.9992$.

The dependence of ϵ'_r on f of the GaP nanosolid has many features similar to that of TiO_2 and $\alpha\text{-Al}_2\text{O}_3$ nanosolids. In practice, the dielectric characteristic of the GaP nanosolid indicates that several polarization modes,

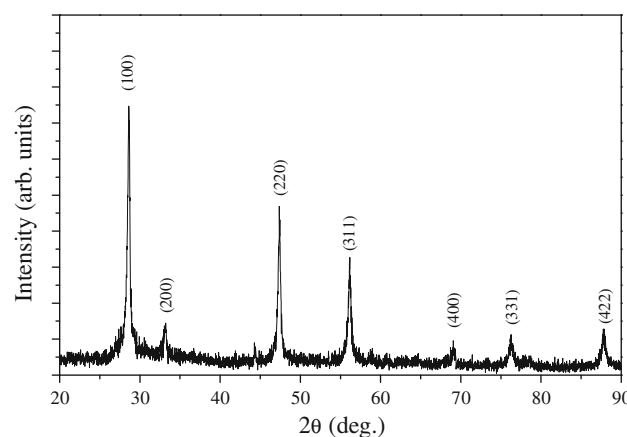


Fig. 1 XRD pattern of GaP nanopowders. The (hkl) values assigned to peaks corresponding to the cubic GaP are in agreement with standard JCPDS values (80-0015)

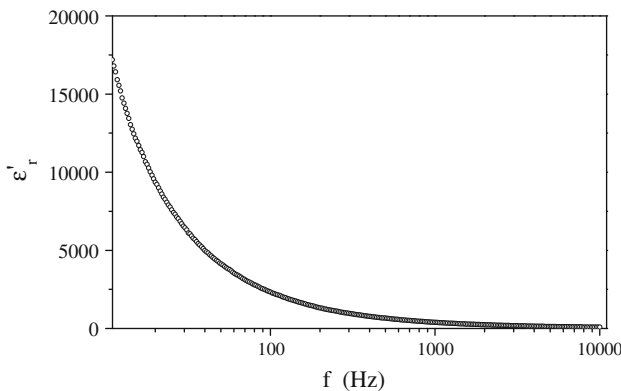


Fig. 2 Values of ϵ'_r of the GaP nanosolid versus f at a temperature of 298 K. When the frequency of alternating voltage increases the value of ϵ'_r at first drastically decreases, and then, begins to drop gradually at high frequencies. A certain critical frequency f_0 when polarization fails to settle itself completely, is not observed

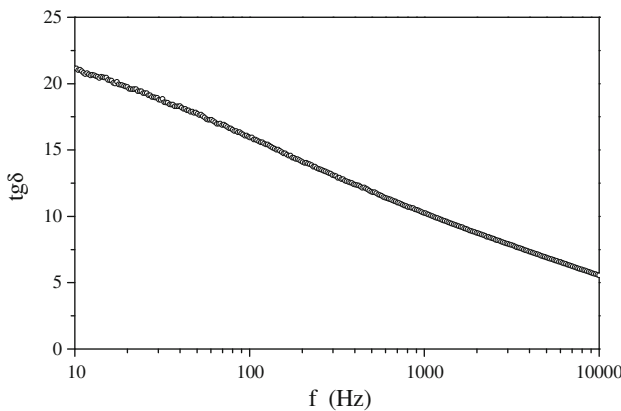


Fig. 3 Values of $\text{tg } \delta$ of the GaP nanosolid versus f at a temperature of 298 K. Owing to the leakage mechanism, the value of $\text{tg } \delta$ is inversely proportional to f , as approximately expressed by Eq. 3

especially interfacial polarization, orientational polarization, and relaxational polarization make an important contribution to the physical essence of the polarization for the GaP nanosolid [7]

The intrinsic point defects of the GaP nanosolid have been investigated by means of electron spin resonance (ESR) [8]. The ESR spectrum attributed to the Ga self-interstitial in the GaP nanosolid was observed with the g value of 2.0028. The concentration of the dangling bonds was evaluated as high as 10^{18} order of magnitude per gram. On the other hand, the GaP nanopowders have the average crystallite size of 50 nm. This nanometric size gives rise to a high number of interfaces. During the compaction process, the free-particle surfaces of the GaP nanopowders were converted into the internal interfaces of the GaP nanosolid, which in the case of a single-phase material were grain boundaries. The great number of interfaces and high density of defects can contribute to the strong dielectric characteristic in the GaP nanosolid.

As we know, bulk GaP is a polar dielectric material. Under the influence of an external electric field, the GaP nanosolid will be polarized. Except for the relaxation polarization mechanism, an important physical essence of the polarization of the GaP nanosolid is the leakage current mechanism. In this case, the complex dielectric permittivity and tangent of dielectric loss angle are given by [9]

$$\epsilon_r^* = \epsilon_{r\infty} + \frac{\epsilon_{rs} - \epsilon_{r\infty}}{1 + i\omega\tau} - i \frac{\gamma}{\epsilon_0\omega} \quad (1)$$

$$\text{tg } \delta = \frac{\frac{\gamma}{\epsilon_0\omega} + (\epsilon_{rs} - \epsilon_{r\infty}) \frac{\omega\tau}{1 + \omega^2\tau^2}}{\epsilon_{r\infty} + \frac{\epsilon_{rs} - \epsilon_{r\infty}}{1 + \omega^2\tau^2}} \quad (2)$$

where ϵ_{rs} , $\epsilon_{r\infty}$, and ϵ_0 are static, high-frequency dielectric constants, and electric constant, respectively; ω is angular frequency ($\omega = 2\pi f$); τ is relaxation time and γ is conductivity. It follows from Eqs. 1 and 2 that the relative dielectric permittivity, the real part of Eq. 1 or denominator of Eq. 2, decreases when the frequency rises, as shown in Fig. 2. And also, the relative dielectric permittivity varies little with the conductivity, γ . As can be seen from Eq. 2, the conductivity, however, has an effect on the tangent of dielectric loss angle. When the leakage current mechanism plays an important role in the physical essence of the polarization, we obtain the dependence of $\text{tg } \delta$ on f in the range of industrial frequency [10]

$$\text{tg } \delta \approx \frac{\gamma}{\omega\epsilon_0\epsilon_{rs}}. \quad (3)$$

In this case, it is apparent that the value of $\text{tg } \delta$ is inversely proportional to f . The experimental results shown in Fig. 3 conform to the sequence established above.

Dependences of ϵ'_r and $\text{tg } \delta$ on T

The dependences of ϵ'_r and $\text{tg } \delta$ on T with various frequencies for the GaP nanosolid are shown in Figs. 4 and 5, respectively. As extrinsic properties, ϵ'_r and $\text{tg } \delta$ depend on the exact size, shape, and microstructure of the specimen. It is easy to see that when the temperature is below about 355 K both $\epsilon'_r(T)$ and $\text{tg } \delta(T)$ curves show maxima near 303 K irrespective of the frequency, but at higher temperature both ϵ'_r and $\text{tg } \delta$ increase gradually with the rise in temperature. The fact that the maxima are fixed at near 303 K irrespective of the frequency does not accord with the feature of the typical dependences for ϵ'_r and $\text{tg } \delta$ of polar substances with a simultaneous change both in temperature and frequency [10]. In terms of the investigation on the local phase transition in GaP by Klimm et al. [4], the presence of such peaks near 303 K can be explained by a local phase transition that can occur in the high hydrostatic stress field of dislocations with an edge component.

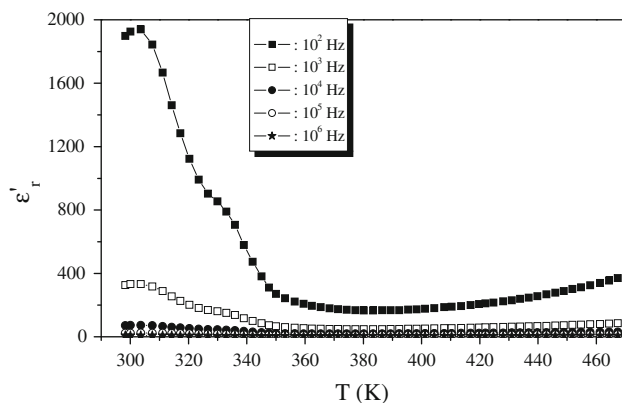


Fig. 4 Values of ϵ'_r versus T with various frequencies for the GaP nanosolid. When the temperature is below about 370 K the $\epsilon'_r(T)$ curves show a maximum near 303 K irrespective of the frequency. For typical polar dielectrics, when the frequency increases the maximum in the temperature trend of ϵ'_r displace toward higher temperatures and become lower. It follows that the maximum near 303 K are different from the dipole maximum caused by the intensification of the chaotic thermal oscillation of molecules and diminution of the degree of orderliness of their orientation

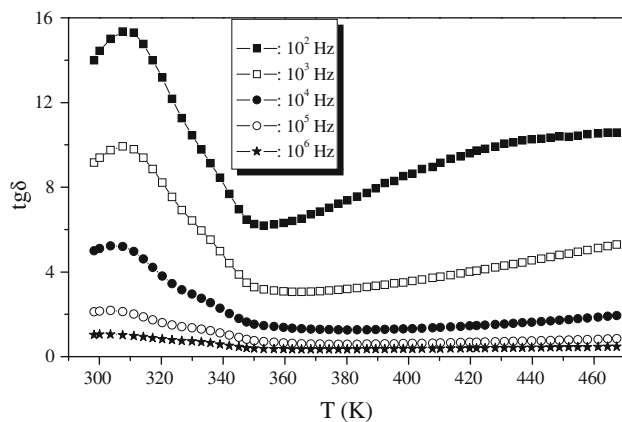


Fig. 5 Values of $\text{tg } \delta$ versus T with various frequencies for the GaP nanosolid. When the temperature is below about 355 K the $\text{tg } \delta(T)$ curves show a maximum near 303 K irrespective of the frequency. For typical dipolar substances, the dielectric losses caused by the dipolar mechanism reach their maximum at a certain definite temperature. When the frequency of alternating voltage increases the temperature corresponding to the maximum of $\text{tg } \delta$ shifts toward higher temperature. Such characteristic sets of curves are not observed for the GaP nanosolids

Local phase transition

Figure 6 shows the typical TEM and HRTEM images of the GaP nanopowders. The particles are subglobular in shape. Because of aggregation, it is difficult to measure the particle sizes of more than a hundred particles of the micrograph. In this case, we could only measure the linear dimension of those particles with sharp contrast along only one direction of micrograph, and the result was averaged. The average

particle size obtained for the GaP nanopowders is about 50 nm. This procedure implies the rotational average as well as the average over the size distribution. Representative HRTEM image reveals that the {111} planes with interplanar spacing of 0.31 nm are visible. The inset shows the enlarged image of the filtered regeneration image of the local region (marked with the arrow). Careful observation of the lattice fringe image indicates the existence of structural defects, such as edge dislocations, in the GaP crystalline core. The dislocation density is proportional to the number of grain boundary ledges and this, in turn, is a function of the grain size. To evaluate the dislocation density, we assume that the GaP nanopowders are spherical with the diameter of 50 nm and only a dislocation line is created in a GaP nanocrystalline. Then, the dislocation density could be conservatively estimated as high as 10^{10} cm^{-2} . Such a high dislocation density means that there exist considerable stress fields of dislocations with an edge component in the GaP nanosolid.

The existence of a stress field around a dislocation means that when an external electric field is applied to GaP crystal an energy gradient will be created for the dislocation [11]. In addition, the electric field may change the shape of the stress field around dislocations [4]. In response to these changes, there is almost always some way in which the structure of the dislocations can change to reduce the total energy. That is, spontaneous and reversible changes of the configuration of the defect responsible for ϵ'_r and $\text{tg } \delta$ maxima may occur at a certain temperature T_c [12].

Under the influence of an external electric field, the Gibbs free energy per unit volume of a mechanically stressed solid near a phase transition temperature T_c can be written in the differential form [11]

$$dg = -sdT - \varepsilon d\sigma - Ad\xi - DdE \quad (4)$$

where s is the entropy per unit volume; ε is the deformation; σ is the stress; A is the affinity; ξ is the order parameter (only one order parameter shall be considered here); D is the electric displacement and E is the intensity of the electric field. Landau has shown that the following ansatz for the solution of Eq. 4 meets the requirements for a phase transition, if $\beta = a(T - T_c)$ [4]

$$g(\sigma, \xi, T, E) = g(0, 0, T, 0) - \frac{1}{2} J_u \sigma^2 - \aleph \sigma \xi - \alpha \sigma \Delta T - \frac{1}{2} \varepsilon_u E^2 - \lambda E \xi + \frac{1}{2} \beta \xi^2 + \frac{1}{4} \gamma \xi^4 \quad (5)$$

where J_u is the unrelaxed compliance; \aleph is the coefficient which measures the coupling between ξ and ε ; α is the thermal expansion coefficient; ΔT is the difference between the temperature T and a selected reference temperature T_0 ; ε_u is the unrelaxed dielectric permittivity and λ is a constant. The terms $-\frac{1}{2} J_u \sigma^2$ or $-\aleph \sigma \xi$ express the elastic and

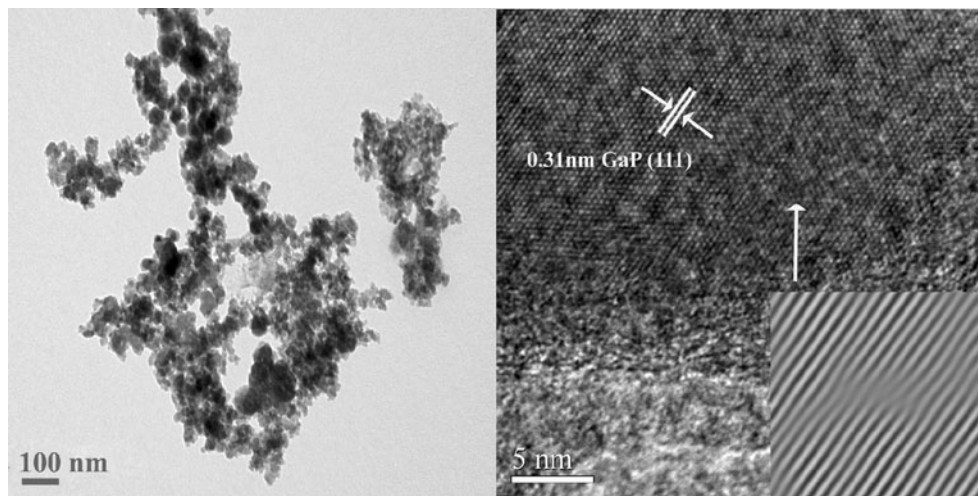


Fig. 6 TEM image and HRTEM image of the GaP nanopowder revealing the atomic structure. The {111} planes with interplanar spacing of 0.31 nm are visible. Structural defects, especially

dislocations, can be observed in the GaP crystalline core. The *inset* shows the enlarged image of the local region (*marked with arrow*), for the sake of observation of dislocations

anelastic contributions to g , respectively. $\alpha\sigma\Delta T$ yields the energy needed to perform linear thermal expansion. The terms $-\frac{1}{2}\epsilon_0 E_{\text{el}}^2$ and $-\lambda E_{\text{el}}\xi$ express the contributions of the external electric field to g .

At a phase transition, g will always be continuous but its derivatives show discontinuities. From Eqs. 4 and 5, we have for the affinity,

$$A = -\left(\frac{\partial g}{\partial \xi}\right) = -\aleph\sigma - \lambda E + a(T - T_c)\xi + \gamma\xi^3. \quad (6)$$

The condition for equilibrium at given stress and external electric field is $A = 0$, or

$$-\aleph\sigma - \lambda E + a(T - T_c)\bar{\xi} + \gamma\bar{\xi}^3 = 0 \quad (7)$$

where $\bar{\xi}$ is the equilibrium value of ξ . Since, from Eq. 4, the entropy per unit volume s is $-\left(\frac{\partial g}{\partial T}\right)$, we then obtain

$$\begin{aligned} s &= s(0, 0, T, 0) - \aleph\sigma\left(\frac{\partial \xi}{\partial T}\right) - \alpha\sigma - \lambda E\left(\frac{\partial \xi}{\partial T}\right) + \frac{1}{2}a\xi^2 \\ &\quad + a(T - T_c)\xi\left(\frac{\partial \xi}{\partial T}\right) + \gamma\xi^3\left(\frac{\partial \xi}{\partial T}\right). \end{aligned} \quad (8)$$

With the aid of Eq. 7, the entropy per unit volume at equilibrium is given by

$$s = s(0, 0, T, 0) - \alpha\sigma + \frac{1}{2}a\bar{\xi}^2 \quad (9)$$

showing that s is dependent on $\bar{\xi}$. Equations 7 and 9 allow for the fact that both $\bar{\xi}$ and s may be functions of temperature, stress as well as external electric field.

To return from the thermodynamic consideration of a mechanically stressed solid to the theme, consider again

the spontaneous and reversible changes of the configuration of the defect in the GaP nanosolid. Without loss of generality, we suppose that there are two configurations of the defect which produces the ϵ'_r and $\text{tg } \delta$ maxima: a high temperature configuration Θ and a low-temperature configuration θ , respectively. Θ would possess the larger formation enthalpy H as well as the larger entropy S . Obviously, at low enough a temperature θ will be the stable configuration. But at some higher temperature the Gibbs free energy of Θ , $G(\Theta)$, may be lower than $G(\theta)$ and the defect will transform to the configuration Θ , as shown in Fig. 7. As already mentioned above, one may consider the entropy per volume at equilibrium as the function of temperature, stress as well as external electric field. It is, therefore, reasonable to expect that the entropy per volume varies between θ and Θ . This points to the entropy-driven metastability [13]. There is a critical temperature, T_c , at which $G(\theta) = G(\Theta)$. Using the thermodynamic equation, $G = H - TS$, the equality, $\Delta H = T_c \cdot \Delta S$, is satisfied. Here, ΔH is the maximum enthalpy change along the path from θ and Θ , and ΔS is the corresponding entropy change. The ratio $k\Delta H/\Delta S = 0.0261 \text{ eV}$ corresponds to a critical temperature of about 303 K, where $k = 1.3806 \times 10^{-23} \text{ J K}^{-1}$ is the Boltzmann constant. In more general sense, it may be noted that the analysis of a configuration change occurring spontaneously and abruptly at a critical temperature by Hamilton et al. allows us to estimate the value of ΔH for entropy-driven phase transition to be probably 0.1 eV [13]. From this result, ΔS would lie in the range $4k - 5k$ and meet the requirements of the local phase transition of the GaP nanosolid.

It has been mentioned that with a sine voltage of $f = 100 \text{ kHz}$ and $U = 10 \text{ mV}$ the dielectric measurements

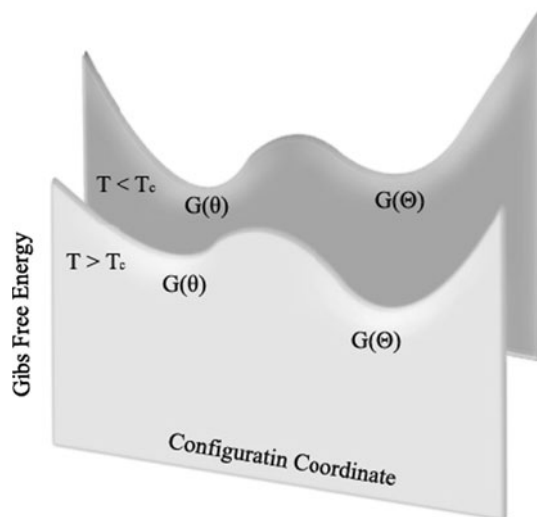


Fig. 7 Schematic diagram of the variation of Gibbs free energy of formation with a generalized coordinate near the local phase transition temperature, T_c . At the temperature lower than T_c , $G(\theta) < G(\thetā)$, θ will be the stable configuration; and at the temperature higher than T_c , $G(\theta) > G(\thetā)$, $\thetā$ will be the stable configuration

were performed by Klimm et al [4]. From the $\epsilon'(T)$ and $\epsilon''(T)$ curves, the transformation temperature of GaP:S after ultrasonic treatment was determined as 303 or 302 K, respectively. In the present experiment, the $\epsilon'_r(T)$ and $\operatorname{tg} \delta(T)$ curves as depicted in Figs. 4 and 5 show maxima at 304 or 303 K, respectively, with the frequency of $f = 100$ kHz. Taking into account of the uncertainties in temperature measurement ($\Delta T = 1\text{--}2$ K), we can arrive at the conclusion that the local phase transition temperature of the GaP nanosolid is approximately equivalent to that of the GaP:S crystal used by Klimm et al. It follows that under the influence of an external field the phase transition temperature T_c at which the local phase transition occurs practically depend upon the nature of the defects.

Conclusions

It can be concluded that the leakage current mechanism plays an important role in the dielectric loss of the GaP

nanosolid. The dielectric characteristic of the GaP nanosolid in the range 298–350 K allows to detect an ϵ'_r or $\operatorname{tg} \delta$ peak at 303 K which can be explained by a local phase transition that can occur in the high hydrostatic stress field of dislocations with an edge component.

Under the influence of an external electric field, the high hydrostatic stress field of dislocations with an edge component of the GaP nanosolid can undergo changes in deformation, accompanied by the drastic stress-induced changes of the order parameter near the phase transition temperature, and hence, changes of Gibbs free energy can be found. In other words, the external electric field affects the dislocation structure. Spontaneous and reversible changes of the configuration of the defects can occur at a critical temperature.

References

1. Robert K, Ian H, Mark G (2007) Nanoscale science and technology (process block). Science Press, Beijing
2. Mohanty J, Hesjedal T, Ney A, Takagaki Y, Koch R, Däweritz L, Ploog KH (2003) *Appl Phys Lett* 83(14):2829
3. Klimm D (1994) *Phys Stat Sol (a)* 143(2):305
4. Klimm D, Klimm C, Banys J (1995) *Phys Stat Sol (a)* 148(2):K69
5. Zhang Zh-Ch, Wang B-P (2009) *Part Part Syst Char* 26(1):53
6. Barker AS Jr (1968) *Phys Rev* 165(3):917
7. Zhang LD, Mou GM (2001) Nanomaterials and nanostrctures. Science Press, Beijing
8. Zhang ZZ, Zou LJ, Cui DL (2004) *Mater Sci Eng B* 111(1):5
9. Li HL (1990) Introduction to dielectrics physics. Press of Chengdu University of Science and Technology, Chengdu
10. Tareev B (1979) Physics of dielectric materials. Mir Publishers, Moscow
11. Nowick AS, Berry BS (1972) Anelastic relaxation in crystalline solids. Academic Press, New York/London
12. Stefański M, Alexander H (1991) *Appl Phys A* 53(1):62
13. Hamilton B, Peaker AR, Pantelides S (1988) *Phys Rev Lett* 61(14):1627